

## 1. INTRODUCTION

Intermediate-velocity clouds (IVCs) have been identified in HI surveys by their emission at large galactic latitudes and at velocities incompatible with a simple model of differential galactic rotation. While their origin has not yet been ascertained, it has been suggested that at least some of the IVCs represent the return flow of a galactic fountain.

We study the physical and chemical properties of the molecular gas in three HI intermediate-velocity clouds. Distance estimates put these clouds in the disk-halo interface with z-heights of typically a few hundred parsecs. Observations of the three lowest rotational transitions of  $^{12}\text{CO}$  and its isotopologue  $^{13}\text{CO}$  are presented. The CO data is complemented by observations of the carbon 492 GHz fine-structure transition made for two of the clouds. We will refer to the molecular clouds detected in the HI IVCs as *intermediate-velocity molecular clouds*, IVMCs.

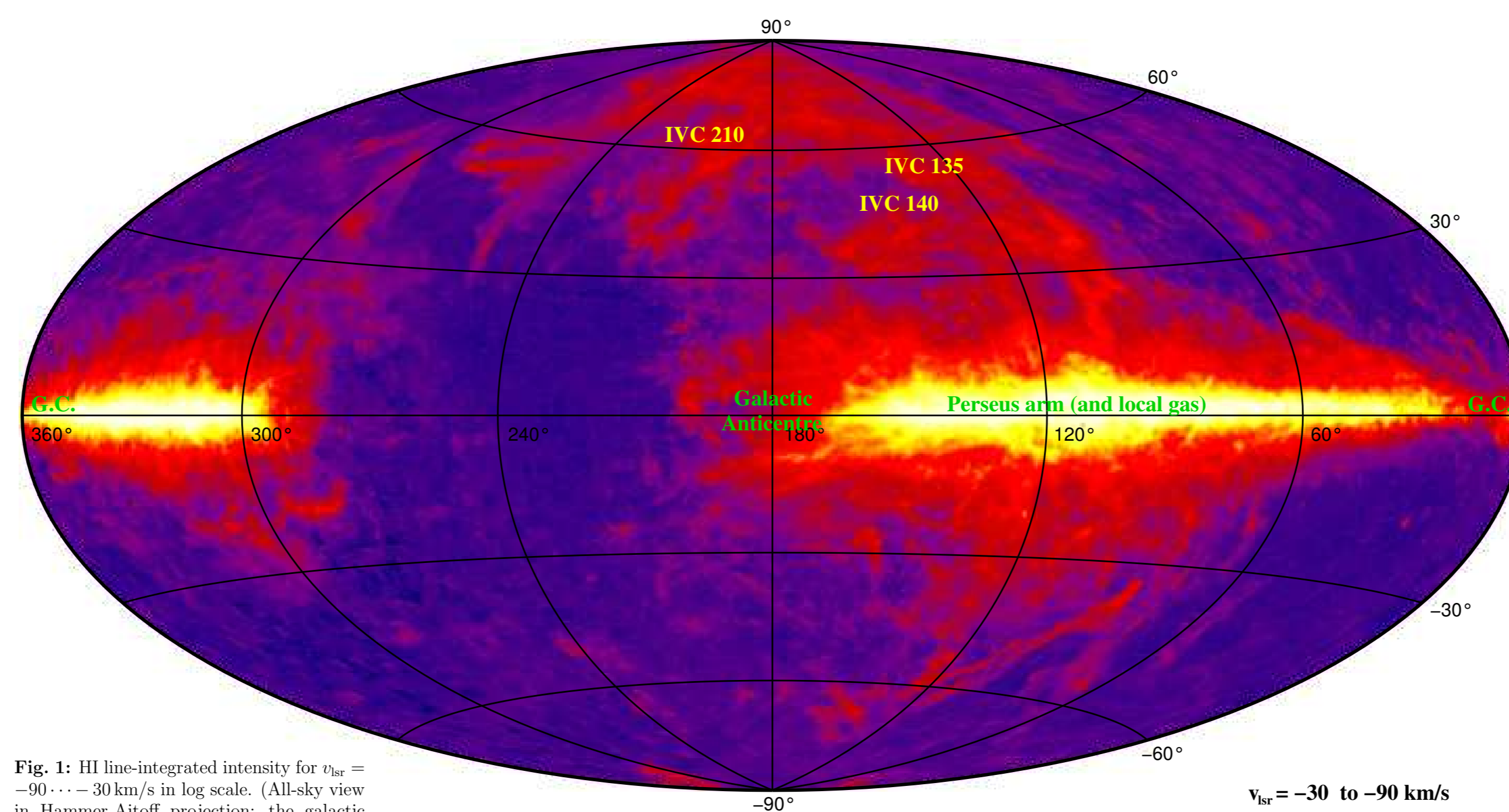


Fig. 1: HI line-integrated intensity for  $v_{lsr} = -90$  to  $-30$  km/s in log scale. (All-sky view in Hammer-Aitoff projection; the galactic anti-centre at  $l = 180^\circ$  is in the middle.) The HI data was taken from the Leiden-Argentine-Bonn HI survey (LAB survey; Kalberla et al., 2005, A&A, 440, 775). The location of the intermediate-velocity clouds studied in the present poster are marked.

## CONCLUSIONS

The intermediate-velocity molecular clouds (IVMCs) traced by CO cover only a small area ( $\lesssim 1$  pc) and the *cloud-averaged* column density of the molecular gas is only a small fraction of the total column density of  $A_v \lesssim 0.1$ . IVMCs therefore might represent regions where  $\text{H}_2$  is being formed. However, the CO line-emitting gas has physical conditions which are similar to those in translucent clouds and cloud surfaces in the Galaxy, and is dominated by small ( $\ll 0.05$  pc) and dense ( $n \approx 10^{3.0} - 10^{4.5}$ ) clumps. This is supported by the PDR models which require small clumps and high densities ( $> 10^4 \text{ cm}^{-3}$ ) to match the observed  $[\text{C}]/\text{CO}$  line ratios. This suggests that if the IVMCs represent regions where molecular gas is formed, this formation proceeds in small clumps  $\ll 0.05$  pc and sufficiently fast to result in carbon, CO abundances and line excitation which are not significantly different from diffuse molecular gas in the galactic disk.

## 2. TARGET CLOUDS

Observations were made for three intermediate-velocity molecular clouds (IVMCs) in the northern hemisphere, located in larger HI IVC clouds/complexes:

name	HI (IVC) complex*	l	b	$v_{lsr}$ (km/s)
IVMC135	IV-Arch (core 21)	135.6	54.3	-46.2
IVMC141	IV-Arch	141.6	48.2	-13.7
IVMC210	IV-Spur	210.9	63.4	-11.6 and -38.2 <sup>†</sup>

\* following Kuntz & Daulay (1996) ApJ, 457, 703.  
† Line profile shows two velocity components, separated by  $\sim 3.5$  km/s

Typical properties of the HI IVCs (see Fig. 2 to the right):

- distance: 130-450 kpc ( $1' \rightarrow 0.04$ - $0.13$  pc);
- distance to galactic midplane: 100-360 pc;
- Visual extinction  $A_v = 0.05 - 0.1$  (at  $8'$  resolution);
- HI column density  $N_{\text{HI}} = (1 - 2) \times 10^{20} \text{ cm}^{-2}$  ( $0.5^\circ$  res.);

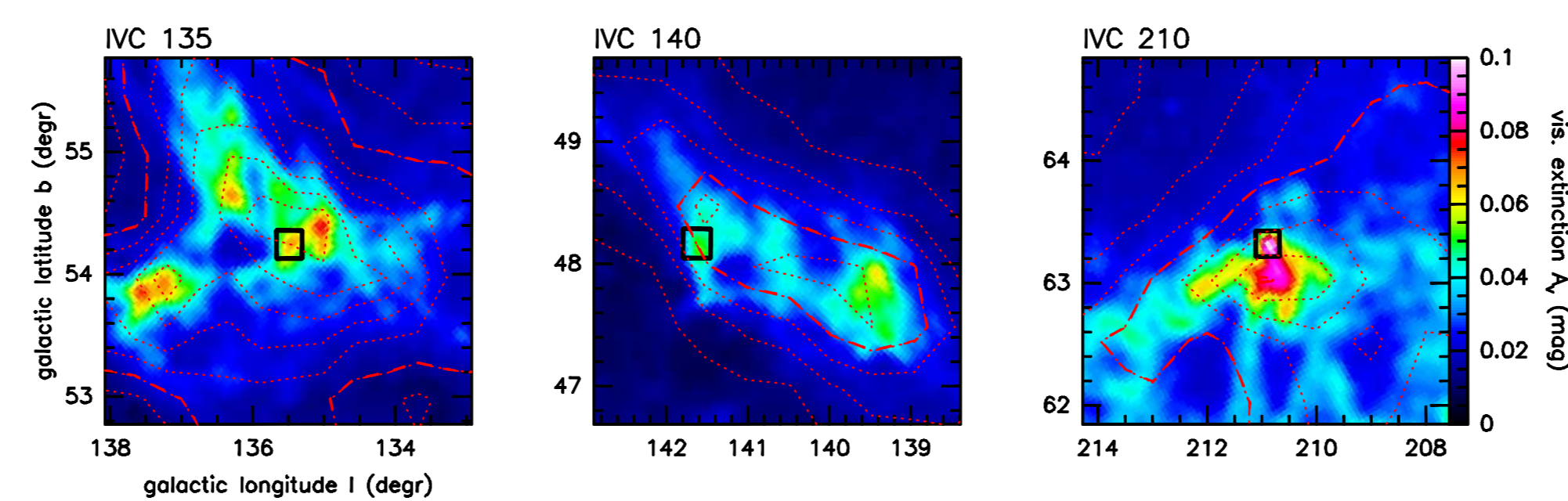
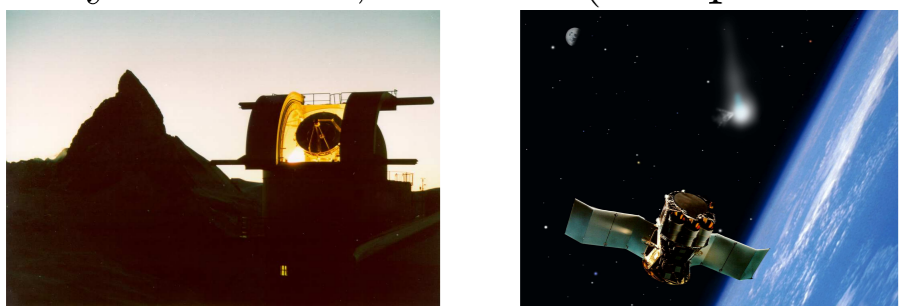


Fig. 2: Maps of the visual extinction (color coded; Schlegel et al., 1998, ApJ, 500, 525) and HI column density (contours; LAB survey) for the HI intermediate-velocity clouds IVC135, IVC140, and IVC210. The column density of  $N_{\text{HI}} = 10^{20} \text{ cm}^{-2}$  is marked by the dashed contour and increments by  $2.5 \times 10^{19} \text{ cm}^{-2}$  for the dotted contours. The regions mapped in CO with the KOSMA 3m telescope (shown in the upper right panel of Figs. 3-5) are highlighted by the dark rectangle.

## 3. OBSERVATIONS

The CO and  $[\text{C}]/\text{CO}$  (sub-)millimetre observations made for each cloud split in two sub sets:

- low-angular resolution data ( $\gtrsim 1'$ ) obtained with the KOSMA 3m telescope and the Submillimeter Wave Astronomy Satellite, SWAS (left panels of Figs. 3-5);



- high-angular resolution data ( $\lesssim 22''$ ) obtained with the Pico Veleta 30m, HHT/SMT 10m, and JCMT 15m telescope (right panels of Figs. 3-5);



### Summary of the spectral-line data

species, transition	telescope*	beam FWHM	data set
<b>IVMC135</b>			
low-angular resolution data			
$^{12}\text{CO}$ J=2-1	KOSMA 3m	130	map (273 positions, 40" sampling)
J=3-2	KOSMA 3m	82	map (273 positions, 40" sampling)
$^{13}\text{CO}$ J=2-1	KOSMA 3m	130	two positions, 40" sampling
$[\text{C}]/\text{CO}$ $^3\text{P}_1 \rightarrow ^3\text{P}_0$	SWAS	258	one position
high-angular resolution data			
$^{12}\text{CO}$ J=1-0	IRAM 30m <sup>b</sup>	22	map (112 positions, 20" sampling)
J=2-1	IRAM 30m <sup>b</sup>	11	map (136 positions, 20" sampling)
J=3-2	HHT 10m <sup>c</sup>	22	2 positions
$^{13}\text{CO}$ J=1-0	IRAM 30m <sup>b</sup>	22	map (136 positions, 20" sampling)
$[\text{C}]/\text{CO}$ $^3\text{P}_1 \rightarrow ^3\text{P}_0$	HHT 10m <sup>c</sup>	16	2 positions
<b>IVMC141</b>			
low-angular resolution data			
$^{12}\text{CO}$ J=2-1	KOSMA 3m	130	map (204 positions, 40" sampling)
J=3-2	KOSMA 3m	82	map (81 positions, 40" sampling)
high-angular resolution data			
$^{12}\text{CO}$ J=1-0	IRAM 30m	22	map (144 positions, 12" sampling)
J=2-1	IRAM 30m	11	map (576 positions, 6" sampling)
$^{13}\text{CO}$ J=1-0	IRAM 30m	22	map (144 positions, 12" sampling)
<b>IVMC210</b>			
low-angular resolution data			
$^{12}\text{CO}$ J=2-1	KOSMA 3m	130	map (261 positions, 40" sampling)
J=3-2	KOSMA 3m	82	map (224 positions, 40" sampling)
$^{13}\text{CO}$ J=2-1	KOSMA 3m	130	cross-cut (17 positions, 40" sampling)
$[\text{C}]/\text{CO}$ $^3\text{P}_1 \rightarrow ^3\text{P}_0$	KOSMA 3m	55	map (45 positions, 28" sampling)
high-angular resolution data			
$^{12}\text{CO}$ J=1-0	IRAM 30m	22	map (144 positions, 12" sampling)
J=2-1	IRAM 30m	11	map (576 positions, 6" sampling)
J=3-2	JCMT 15m	14	map (81 positions, 10" sampling)
$^{13}\text{CO}$ J=1-0	IRAM 30m	22	map (144 positions, 12" sampling)

Fig. 3-5 show the  $^{12}\text{CO}$  J=2 $\rightarrow$ 1 line-integrated maps and the line profiles toward selected positions.

### Line ratios

The CO line ratios are used to constrain the excitation conditions (temperature, density, column density) of the line-emitting gas and the  $[\text{C}]/\text{CO}$  ratios are compared to a photo-dissociation region (PDR) model ( $\rightarrow$  Sec. 4):

cloud (velocity component)	J=2-1/J=1-0	J=3-2/J=2-1	$[\text{C}]/\text{CO}$ J=2-1	$[\text{C}]/\text{CO}$ J=3-2
IVMC135	0.73 $\pm$ 0.10	0.40 $\pm$ 0.07	0.22 $\pm$ 0.19	0.48 $\pm$ 0.07
IVMC141	0.84 $\pm$ 0.65	0.52 $\pm$ 0.19		0.44 $\pm$ 0.28
IVMC210 (-42 km/s)	0.86 $\pm$ 0.13	0.45 $\pm$ 0.11	0.27 $\pm$ 0.20	0.44 $\pm$ 0.28
IVMC210 (-38 km/s)	0.69 $\pm$ 0.14	0.43 $\pm$ 0.10	0.35 $\pm$ 0.28	0.50 $\pm$ 0.16
Galactic translucent and dark clouds:				
MCLD123.5+24.9 (translucent cloud)	0.63 $\pm$ 0.10	0.39 $\pm$ 0.07	0.14 $\pm$ 0.04	0.37 $\pm$ 0.13
B5 dark cloud edge	0.63 $\pm$ 0.25	0.44 $\pm$ 0.09	0.17 $\pm$ 0.03	0.38 $\pm$ 0.06
B5 dark cloud core	1.16 $\pm$ 0.47	0.83 $\pm$ 0.15	0.14 $\pm$ 0.04	0.17 $\pm$ 0.02

IVMCs and the molecular gas in translucent/diffuse clouds in the Galactic disk have similar CO line ratios.

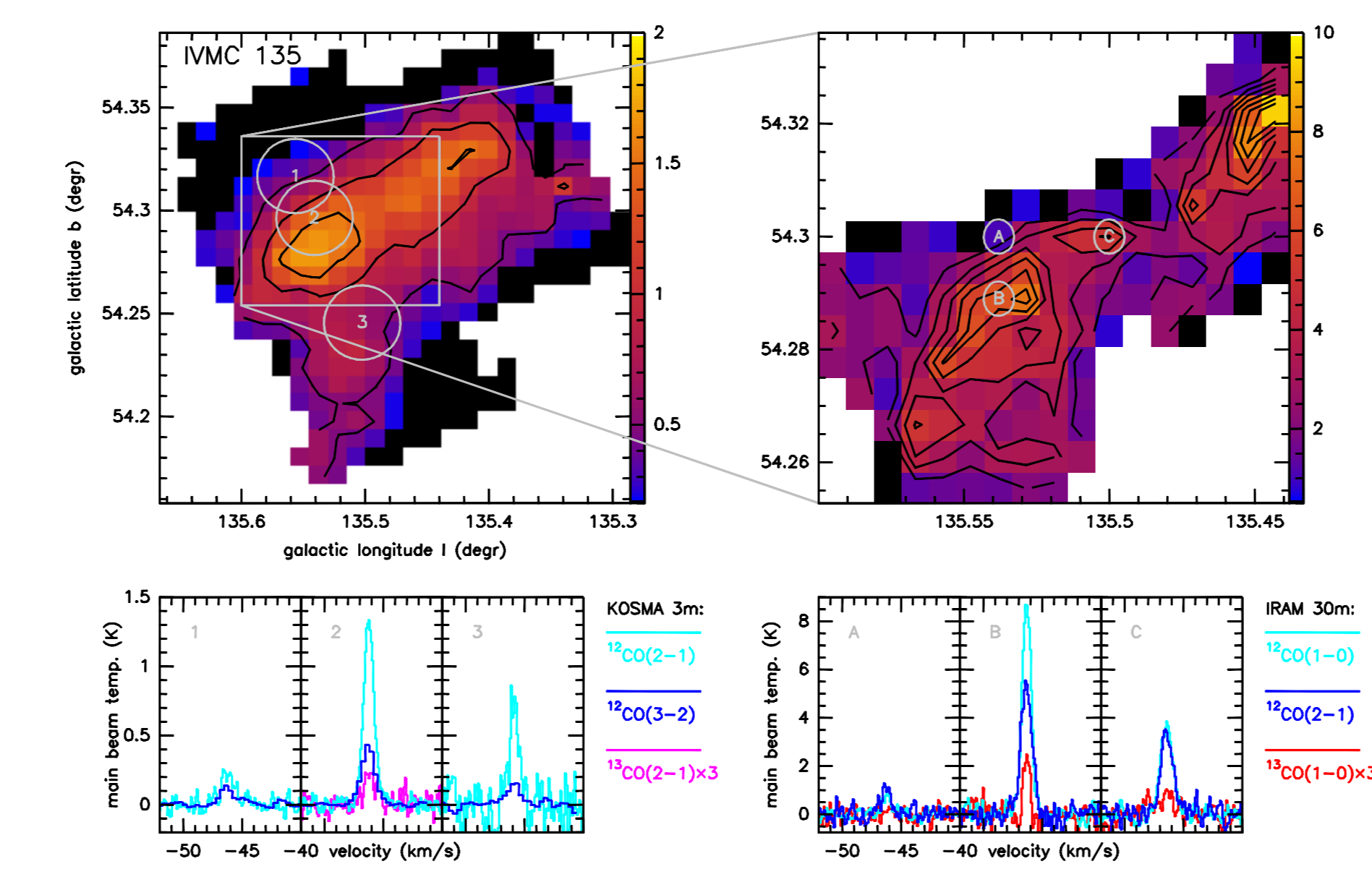


Fig. 3: IVMC135: line-integrated intensity map for the  $^{12}\text{CO}$  J=2 $\rightarrow$ 1 observations made with the KOSMA 3m telescope (top left panel) and Pico Veleta 30m telescope (top right). Line profiles are shown for three selected positions in each map. The position are marked by numbers (letters) in the upper panels, with the circle indicating the main beam FWHM of the telescope.

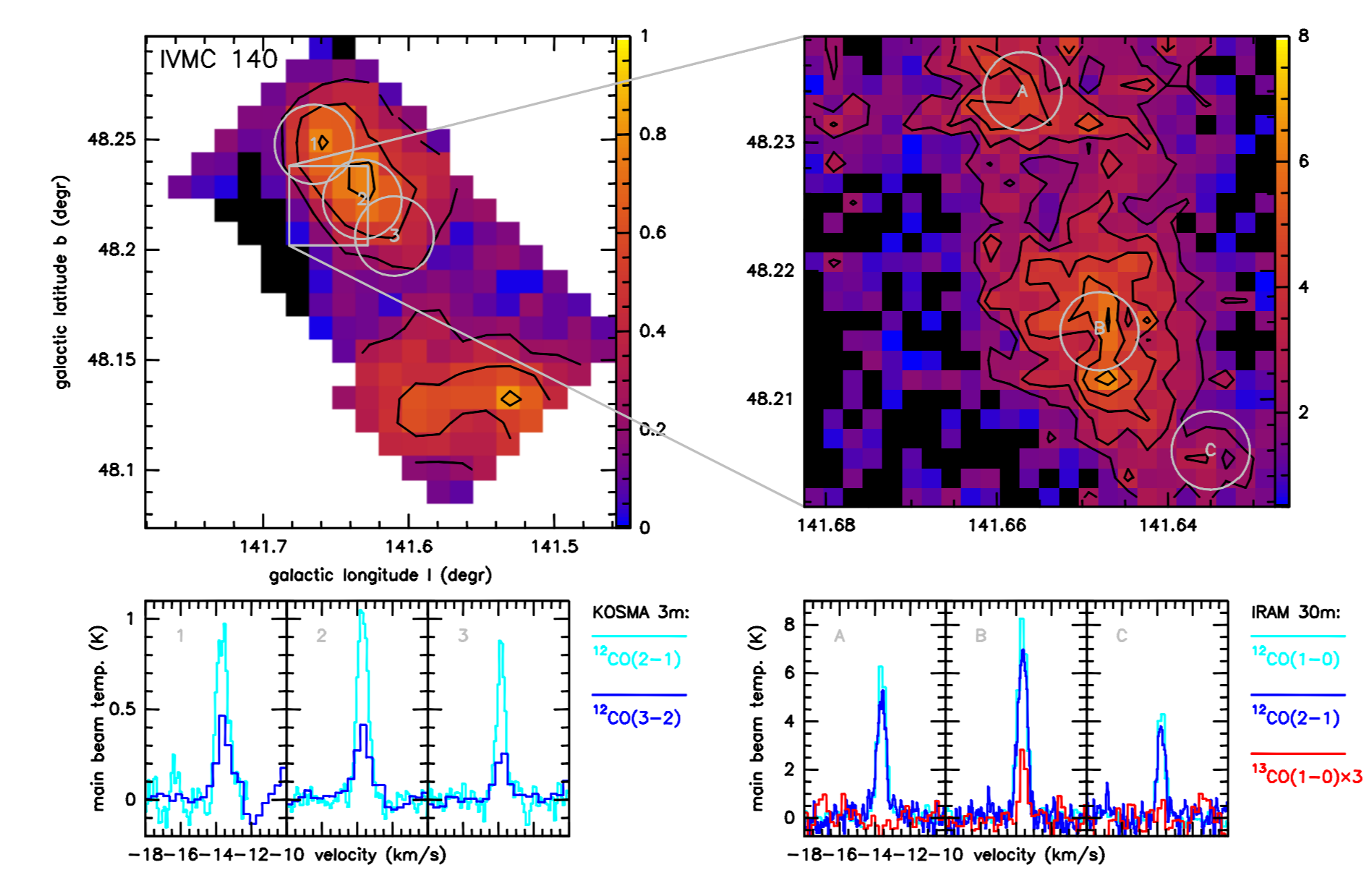


Fig. 4: Same as Fig. 3 for IVMC141

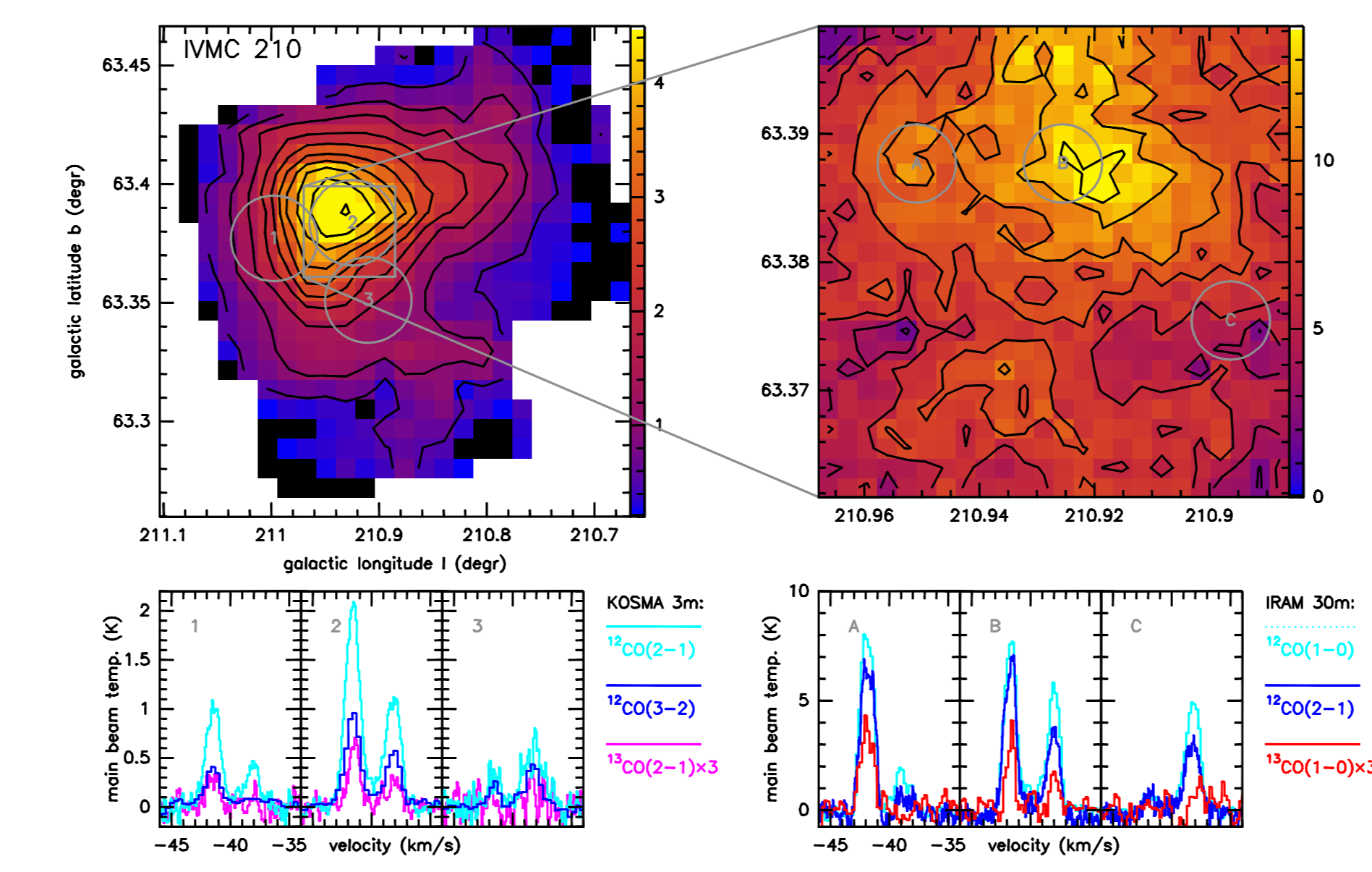


Fig. 5: Same as Fig. 3 for IVMC210

## 4. RESULTS

### Physical properties of the gas traced by CO

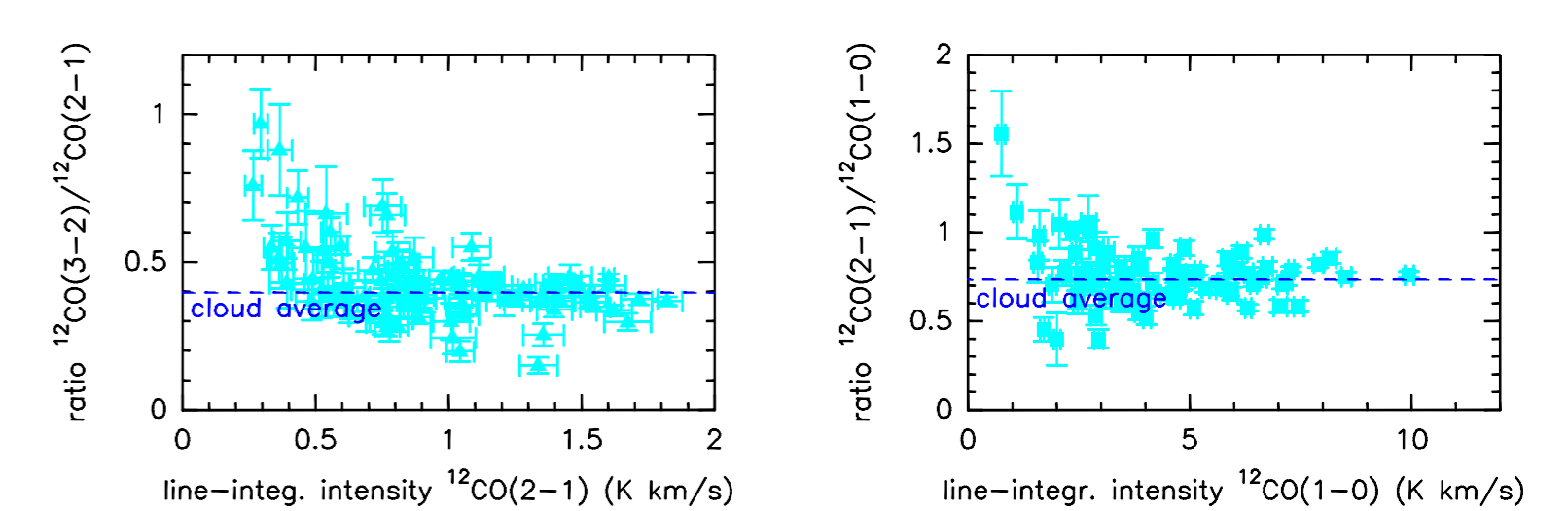
The gas temperature is  $\sim 10 - 16$  K, similar to the temperature measured in galactic molecular clouds remote from strong FUV sources.

- The  $^{12}\text{CO}$  2-1/1-0 ratio is consistent with LTE,  $T_{\text{kin}} \approx 8 - 16$  K.
- The  $^{12}\text{CO}$  1-0 and 2-1 line-peak temperatures measured with the 30m telescope in the *position with the brightest CO emission* gives  $T_{\text{kin}} \gtrsim 11.5$  K.
- The  $^{12}\text{CO}$  line profiles toward the region with strong CO emission are flat topped. This indicates large optical depths, LTE excitation, and a beam filling factor of  $\sim 1$ .

The CO line-emitting regions ('clumps') are much smaller than the telescope beam ( $\ll 0.05$  pc) and a large number of such clumps are sampled in the beam.

- Low beam-averaged column densities of  $N_{\text{CO}} \sim 10^{15.0} - 10^{16.5} \text{ cm}^{-2}$  are derived from the  $^{13}\text{CO}$  observations  $\rightarrow$  even the  $^{12}\text{CO}$  emission is expected to have low to moderate optical depths for positions away from the emission peaks.
- The  $^{12}\text{CO}$  3-2/2-1 ratio is below the LTE ratio at  $T = 10$ - $16$  K.

The  $^{12}\text{CO}$  line ratios are therefore expected to vary with column density *and* density. A plot of the CO line ratio vs. CO line intensity ( $\rightarrow$  proxy for the *beam-averaged* CO column density) shows little to no variation, however; example:  $^{12}\text{CO}$  ratio in IVMC 135:



This suggests that the line-emitting gas in the CO peak *and* in regions with weak CO emission have similar properties (temperature, density, and column density) despite different *beam-averaged* column densities.  $\Rightarrow$  Line emitting regions = clumps  $\ll$  beam, but with a different number of clumps sampled in the beam for both regions.

The comparison of the line ratio to an escape probability model implies  $n \approx 10^{3.0} - 10^{4.5}$  (for  $T_{\text{kin}} \approx 10$ - $16$  K). The figure below compares observations and results from the escape probability model by Stutzki & Winnewisser (1985, A&A, 144, 13). We assume that the line-of-sight extent of the gas is much smaller than the projected main beam FWHM of the 30m telescope ( $d \ll 0.05$  pc; the line emitting regions are not "edge-on" pancakes or "pencil clouds" pointing towards us). This gives an upper limit on the ratio  $N_{\text{CO}}/n \ll x_{\text{CO}} \times d \approx 2.16 \times 10^{13} \text{ cm}$ , for a CO abundance of  $x_{\text{CO}} \approx 1.4 \times 10^{-4}$ .

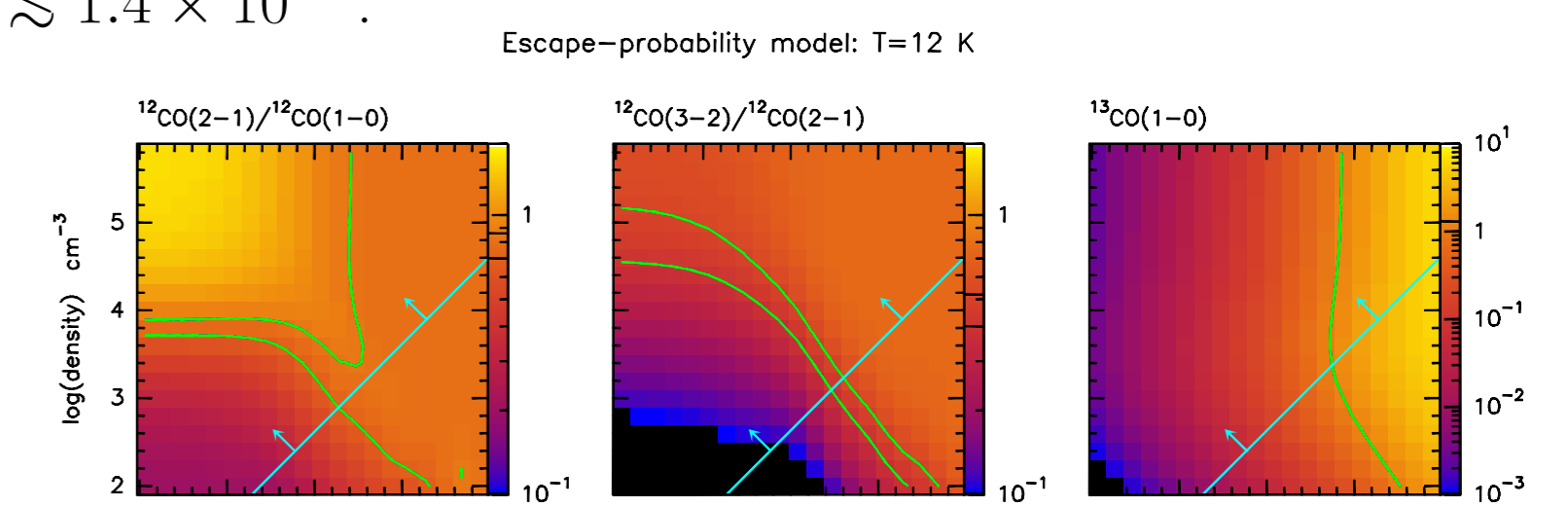


Fig. 7: The green contours bracket the range of CO line ratios observed in the IVMCs (left and middle panel) and gives an upper limit to the  $^{12}\text{CO}$  J=1-0 temperature (= peak temperature in the region with the brightest  $^{12}\text{CO}$  emission; right panel). The region below and to the right of the blue line is excluded based on geometry arguments ( $N_{\text{CO}}/n < 2.16 \times 10^{13} \text{ cm}$ ).

$\Rightarrow$  The models with the best match to the observations have  $n \approx 10^3 - 10^{4.5} \text{ cm}^{-3}$ .

### PDR Modeling

The comparison of the  $[\text{C}]/\text{CO}$  line ratios observed in IVMCs to ratio calculated from a photo-dissociation region model suggests:

- FUV radiation field with an intensity of  $\chi \sim 1 \times \chi_0$ ;
- densities of  $n \gtrsim 10^4 \text{ cm}^{-3}$ ;
- a diffuse (low density) envelope with a  $\text{H}_2$  column density of  $\sim 5 \times 10^{19} \text{ cm}^{-2}$  (a substantial fraction of the total molecular gas column density !);